ELSEVIER

International Journal of Heat and Fluid Flow 21 (2000) 221–227

International Journal of HEAT AND FLUID FLOW

www.elsevier.com/locate/ijhff

Influence of fin spacing and rotational speed on the convective heat exchanges from a rotating finned tube

Barbara Watel [a,*], Souad Harmand [b,1], Bernard Desmet [b,1]

[a] CRT-GRETH, CEA-Grenoble, 17 rue des Martyrs, F-38054 Grenoble Cedex 9, France

[b] LAMIH, Laboratoire de Mécanique et d'Energétique, ENSIMEV, Université de Valenciennes et du Hainaut–Cambrésis, B.P. 311, F-59304 Valenciennes Cedex, France

Received 26 April 1999; accepted 27 September 1999

Abstract

The convective heat transfer from fins to air at rest has been evaluated for rotating annular fins. The fin cooling is studied using infrared thermography. The heat transfer coefficient can be obtained from a fin's thermal balance, during its cooling process and its temperature–time evolution. The influence of the fin rotational speed and the fin spacing on the convective exchanges is studied. The tests were carried out for rotational Reynolds numbers (based on the shaft diameter and the shaft peripheral speed) ranging from 400 to 30 000, for different fin spacings. A correlation of the experimental data has been found. The relative influences of the rotational forced convection and the gravitational natural convection on the heat transfer from the fin surface have also been analyzed.

Keywords: Heat transfer; Natural convection; Forced convection; Rotating fins; Annular fins; Fin spacing

Notation

C	specific heat at constant pressure (J/kg K)
D	tube outer diameter (m)
d_{eff}	effective diameter ($=D+H_a$) (m)
E	fin efficiency
e	fin thickness (m)
e'	dimensionless fin thickness ($=e/D$)
Gr_g	Grashof number ($=g\beta\Delta T D^3/\nu_a^2$)
Gr_{gL}	Grashof number ($=g\beta\Delta T L^3/\nu_a^2$) ($L$: dimension of reference)
H_a	fin height ($=R_e-R_i$) (m)
H'	dimensionless fin height ($=H_a/D$)
h_0	mean heat transfer coefficient of the tube surface between fins (W/m^2 K)
h_1	mean heat transfer coefficient of a smooth tube (W/m^2 K)
h_m	mean heat transfer coefficient of fin (W/m^2 K)
h_{red}	reduced heat transfer coefficient of a finned tube (W/m^2 K)
L	tube length (m)
l_{eq}	equivalent length of the disk surface (m)
N	rotational speed (rev/min)
Nu	Nusselt number on the fin ($=\varphi_c D/((T_s-T_\infty)\lambda_a)=h_m D/\lambda_a$)
Nu_1	Nusselt number on the cylinder ($=h_1 D/\lambda_a$)
Nu_L	Nusselt number ($=\varphi_c L/(\Delta T\lambda_a)$) ($L$: dimension of reference)
Pr	Prandtl number ($=\mu_a C_a/\lambda_a$)
R_d	right horizontal radius on the fin a_3
R_e	fin outer radius (m)
Re_H	peripheral Reynolds number ($=\omega R_e^2/\nu_a$)
Re_ω	Reynolds number ($=\omega R_i D/\nu_a$)
R_g	left horizontal radius on the fin a_3
R_i	outer radius of the tube (m)
s	fin pitch (m)
S_a	fin surface in contact with the air ($=(2\pi(R_e^2-R_i^2)+2\pi R_e e)L/s$) (m^2)
S_H	interdisk spacing to disk radius aspect ratio ($=u/R_e$)
S_t	surface of the finned cylinder between the fins ($=\pi DuL/s$) (m^2)
S_1	smooth cylinder surface ($=\pi DL$) (m^2)
T_0	temperature on surface S_t (K)
T_f	air film temperature ($=(T_s+T_\infty)/2$) (K)
T_s	fin surface temperature (K)
U	superposed air flow velocity (m s^{-1})
u	fin spacing (m)
u'	dimensionless fin spacing ($=u/D$)
β	thermal expansion coefficient (K^{-1})
ΔT	temperature difference ($=T_s-T_\infty$) (K)
λ	thermal conductivity (W/m K)
ν	kinematic viscosity (m^2/s)

* Corresponding author. Fax: +33-04-76-85-15-53.
E-mail address: greth@cea.fr (B. Watel).
[1] Fax: +33-03-27-14-79-31.

0142-727X/00/$ - see front matter
PII: S0142-727X(99)00070-3

ρ	density (kg/m^3)
φ_c	convective heat flux (W/m^2)
ϕ_T	total convective heat flow (W)
ω	rotational speed (rad/s)

Subscripts

a	air
al	aluminum
∞	outside the boundary layer

1. Introduction

The research presented here is the continuation of the study of the thermal behavior of the heat-pipe brake disk with a finned tube condenser during the braking phase (Watel et al., 1994, 1995). This first study showed the efficiency of the heat-pipe brake disk in evacuating the heat generated during braking from the condenser's fins when compared with the standard solid disk. The heat transfer coefficient on the fins with the air is necessary for the heat flux boundary conditions on the condenser wall in contact with the air. The evaluation of the convective exchanges from the surface of a rotating fin, for different fin spacings, will lead to a more accurate prediction of the temperatures in the condenser wall and the fin spacing to choose in order to obtain the best cooling of the disk. The heat transfer study of the rotating finned cylinder is also relevant to magnetic disk storage systems, which are pertinent to the computer industry and the cooling of electrical machinery. Fins improve cooling by increasing the surface area available for heat dissipation. More importantly, the presence of fins creates nonuniformities in the flow, setting up secondary vortices. The basic cross-stream flow pattern between two coaxial disks co-rotating in a fixed cylindrical enclosure can be inferred from different authors' analyses (Stewartson, 1957; Murthy, 1988; Chang et al., 1989; Schuler et al., 1990). The basic cross-stream flow pattern consists of two symmetrical and counter-rotating toroidal vortices driven, respectively, by the outflows along the Ekman layers on the two disk surfaces (Fig. 1). These studies also show that the cross-stream vortex pair formed in the $(x-r)$ plane does not fill the entire interdisk space for small values of interdisk spacing to disk radius aspect ratio, S_H. Instead, for $r < R_{cr}$, there is a region surrounding the hub, called the "inner region", where the flow is essentially in solid-body rotation. The symmetrical vortex pair is stable up to a critical value of the Reynolds number $Re_H = \omega R_e^2/\nu_a$, at which point the 2D (axisymmetrical) flow becomes unsteady and 3D (asymmetrical with respect to the interdisk plane). By using a (Re_H, S_H) map, Herrero et al. (1999) showed that the 3D unsteady flow was obtained for high interdisk spacing to disk radius aspect ratio S_H or for high Re_H, whereas the 2D steady flow was obtained for low Reynolds numbers Re_H and low to moderate S_H. For a 3D flow, Akhmetov and Tarasov (1987) and Abrahamson et al. (1989), observed that the flow field consisted of a 2D core sandwiched between thin, 3D boundary layers on each disk. The core can be divided into three distinct regions (Fig. 2). The inner region boundary is polygonal. Lennemann (1974) observed that the inner region boundary was oval in a plane parallel to the fins when the separation distance between the edge of the fins and the shroud approached infinity. The "outer region", dominated by large vortical structures whose vorticity is counter-aligned with the spin axis of the fins, is between the inner region and the disk periphery. The absolute rotational speed of the train of vortices distributed around a circle is equal to about 75% of the fin speed. This region is much more actively turbulent than the inner region. These outer region vortices give a polygonal shape to the inner region. A regular fluid exchange between these two regions occurs. The third region is the boundary layer on the shroud. All the authors quoted previously worked on annular fins rotating inside a stationary shroud, which does not correspond to our experimental device.

The VDI-Wärmeatlas (1991) and Hahne and Zhu (1994) give correlations for heat transfer by natural convection from a tube with annular fins. In the literature, however, no article was found which dealt with heat transfer from annular fins of a finned tube rotating in free flow without a shroud.

The convective exchanges from a rotating finned tube, subjected or not to an air flow parallel to the fins' surface, have been evaluated for only one fin spacing, $u = 2$ mm, in a previous study (Watel et al., 1998). The purpose of the present work is to continue this research by carrying out new tests for different fin spacings. It also aims to analyze the influence of the fin spacing and the rotational speed on the convective heat transfer to the air from circular rotating fins, without any superposed air flow, within the Reynolds number range $400 < Re_\omega < 30\,000$. The experimental method used to determine the mean convective heat transfer from the fin surface from the temperature time variation of the fin is outlined in the first part. Tests were carried out within the dimensionless fin spacing range $0.034 < u' < 0.69$ and for a single fin mounted on the tube (corresponding to $u' = \infty$). For all the tests, the Grashof number is estimated at $Gr_g = 1.35 \times 10^6$. In our tests, the convective heat transfer from the surface of rotating fins is controlled by dimensionless numbers Re_ω and Gr_g expressing the exchanges by rotational forced convection and the phenomena of gravitational natural convection, respectively. The

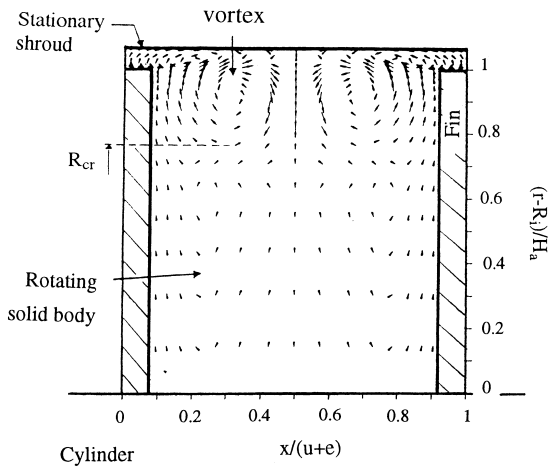

Fig. 1. Cross-stream vector velocity field (compressed in radial direction) (Chang et al., 1989).

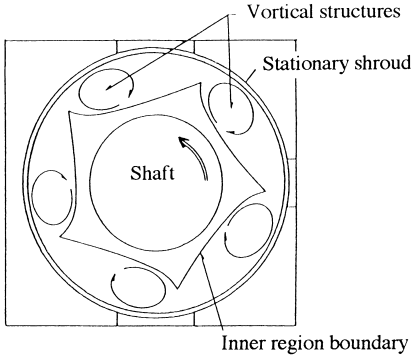

Fig. 2. Sketch of the flow structure in the midplane between the fins (Abrahamson et al., 1989).

purpose of this work is also to correlate all the tests with an equation that expresses the average Nusselt number on the fin as a function of dimensionless fin spacing u', of rotational Reynolds number Re_ω and of Grashof number Gr_g. The correlation obtained evaluates the influence of gravitational natural convection and rotational forced convection on the convective exchanges.

It is interesting to compare the total convective heat transfer from the finned tube surface with that from the isolated cylinder, for different fin spacings and Reynolds numbers.

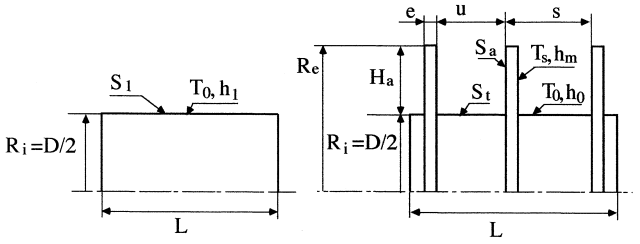

Fig. 4. Finned tube geometry.

2. Experimental method

The experimental method and its validation have been described in detail in a previous article (Watel et al., 1998). The convective exchanges from the surface of an annular fin are obtained by measuring its temperature–time evolution. The temperature is measured on the central fin a_3 of a tube which has five fins (inner radius R_i, outer radius R_e) (Fig. 3). During the tests, the finned tube is placed inside a casing of a rectangular cross-section (0.4×0.3 m^2). A radiant panel emitting short infrared waves is placed horizontally above the fins and uniformly heats them to temperatures ranging from 110°C to 140°C. After the heating interruption, the central fin's a_3 cooling is studied by infrared thermography (THERMOVISION® 900 system, type 900 SW/TE), in line scanning mode. The camera, whose optical axis is merged with the rotational axis of the finned tube, is placed so that the line scanning occurs along the horizontal diameter of the fin. The tunnel's vertical wall has two rectangular slits f_{pg} and f_{pd} and the fins a_1 and a_2, placed between the fin a_3 and the tunnel wall, have a rectangular slit along the whole length of their radius (f_1 and f_2). The camera can therefore visualize the horizontal radii R_g and R_d on the fin a_3, when the portion r_3 is in front of rectangular slits f_{pg} and f_{pd}, respectively (Fig. 3), and the temperature distribution is obtained along radii R_g and R_d of fin a_3.

The fins ($R_e = 50$ mm, $H_a = 21$ mm, $e = 1$ mm, corresponding to dimensionless parameters $H' = 0.362$ and $e' = 0.017$) are made of aluminum ($\rho_{al} = 2720$ kg m^{-3}, $\lambda_{al} = 233$ W m^{-1} K^{-1}, $C_{al} = 0.98$ kJ kg^{-1} K^{-1}) (Fig. 4). The suitable fin spacing u is obtained through insulating rings (of various thicknesses $u = 2$, 3, 4, 6, 14 or 40 mm, $D = 58$ mm).

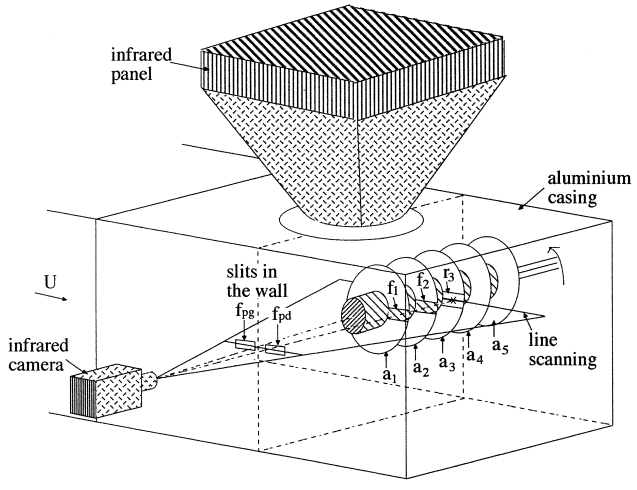

Fig. 3. Schematic representation of the test facilities.

Furthermore, tests are carried out with a single fin mounted on the tube. The fins and rings are covered with a thin coat of black paint. Making the fins from a highly conductive metal and coating their surface with a high emissivity paint means that the fins all absorb the same amount of heat and their temperatures remain identical during the cooling process. Moreover, the fin's temperature remains relatively uniform during the cooling process. Indeed, it is deduced from the temperature distribution along horizontal radii R_g and R_d of the fin a_3 that ratio $(T_{min} - T_\infty)/(T_{max} - T_\infty)$ remains equal to about 0.95, whatever instant t is during the cooling phase; $T_{max}(r)$ and $T_{min}(r)$ are, respectively, the maximum and minimum temperatures obtained on a radius. Moreover, the temperature distribution at instant t is the same on radius R_g and radius R_d. Indeed, under the effect of the rotation and thanks to the high aluminum thermal conductivity, the temperature distribution tends to have a revolution symmetry. A correct value of the fin's temperature is therefore given by the arithmetic mean of the temperatures obtained on a radius of the fin.

For the tests, the finned tube rotational speed can be varied between 50 and 3200 rpm. As shown in Fig. 3, a flow of very low velocity U is driven through the apparatus in order to air the casing. It has been proved that, as the ratio $U/\omega R_i$ remains lower than 0.1, the influence of this superposed air flow is negligible on the convective heat transfer when compared to the rotational convection. A thermocouple is placed at the center of the wind tunnel test section which is 80 mm upstream of the fins. The maximum variation of the air temperature during a test is 1°C and the time average value T_∞ is used as a reference temperature in the Nusselt number.

The energy equation integrated in the fin in a fixed time interval during the cooling then leads to the mean heat transfer coefficient of the fin h_m deduced from its temperature time evolution. The relative error on h_m is a decreasing function of the rotational speed. For our tests, it is between 8% (obtained for $N = 3200$ rpm) and 25% (obtained for $N = 50$ rpm). In order to check that the slits in the fins a_1 and a_2 do not affect the convective heat transfer, present test results obtained for the lowest Reynolds numbers, are compared with correlations given by different authors for heat transfer by natural convection from a tube with annular fins (see Section 3.1).

3. Results and discussion

The physical properties and thermal expansion coefficient in the numbers Nu, Re_ω and Gr_g are evaluated at the air film temperature T_f. The test results are plotted in Fig. 5, under the form $Nu = f(Re_\omega)$, for rotational speeds between 50 and 3200 rpm ($400 < Re_\omega < 30\,000$) and for different dimensionless spacings u' between 0.034 and 0.69, as for the tube with a single fin. The mean value of the Grashof number is $Gr_g = 1.35 \times 10^6$, for all the tests.

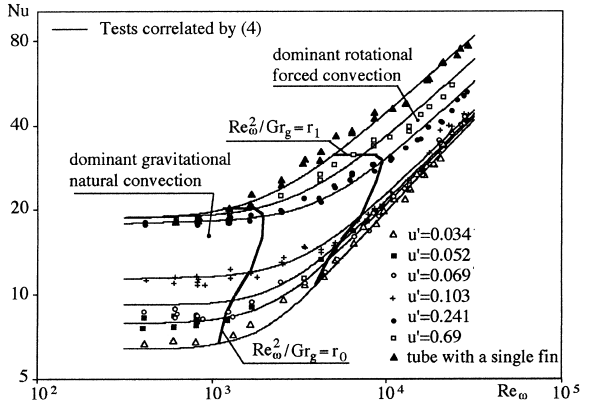

Fig. 5. Test results with rotation and correlation ($Gr_g = 1.35 \times 10^6$).

3.1. Analysis of the tests carried out with dominant gravitational natural convection

Among the tests carried out with the rotating fins and plotted in Fig. 5, only those with a predominant influence of gravitational natural convection on the convective exchanges when compared with rotational convection are studied in this section. For each spacing, these are the tests carried out with the lowest rotational speeds, for which the heat transfer coefficient is independent of the rotational speed. In this case, the flow structure close to the fins is similar to that obtained on fixed fins by natural convection, though these tests have been carried out with Reynolds numbers Re_ω higher than 400. For each spacing, the arithmetic mean of the Nusselt numbers for tests located in the region of predominant influence of gravitational natural convection ($Gr_g = 1.35 \times 10^6$) is shown in Fig. 6 as a function of dimensionless spacing u'. The Nusselt number increases with fin spacing and becomes equal to the asymptotic value $Nu = 18.5$ from $u' \approx 0.26$. This value corresponds to the Nusselt number obtained on an isolated fin cooled by natural convection. The upward fluid flow by natural convection is made easier with the increase in u' because the temperature gradients in the fluid are higher. This allows the boundary layers to develop without interference on two adjacent fins and explains the increase in the Nusselt number as u' increases. u' has little influence on Nu as there is no more interaction of the boundary layers on two adjacent fins. Fig. 6 shows that this occurs when $u' > 0.26$. Our tests carried out with a preponderance of gravitational natural convection are

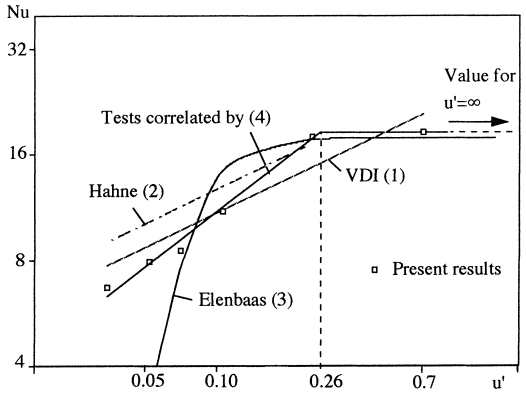

Fig. 6. Comparison of the test results by natural convection with the bibliography ($Gr_g = 1.35 \times 10^6$).

accurately correlated by Eq. (4), in which Re_ω is equal to 0, since its influence on Nu is negligible for these tests.

Our results have been compared to the correlations respectively proposed by the VDI-Wärmeatlas (1991) and Hahne and Zhu (1994) to calculate the average heat transfer coefficient h_m at the surface of a fixed tube including vertical annular fins cooled by natural convection. The correlation proposed by the VDI-Wärmeatlas (1991), with $a \pm 25\%$ accuracy is valid for $10^3 < Gr_{gd_{eff}} Pr < 10^7$, with $d_{eff} = D + H_a$:

$$Nu_{d_{eff}} = 0.24(Gr_{gd_{eff}} Pr\, u/D)^{1/3}. \quad (1)$$

Hahne and Zhu (1994) obtained the following correlation experimentally, in the range $5 \times 10^4 < Gr_{gd_{eff}} Pr\, u/D < 5 \times 10^5$:

$$Nu_{d_{eff}} = 0.28(Gr_{gd_{eff}} Pr\, u/D)^{1/3}. \quad (2)$$

Eqs. (1) and (2) are plotted in Fig. 6 under the form $Nu = f(u')$, by using $Gr_g = 1.35 \times 10^6$, $D = 58$ mm and $d_{eff} = 79$ mm, with $Nu = Nu_{d_{eff}}(D/d_{eff})$ and $Gr_g = \mathrm{Gr}_{gd_{eff}}(D/d_{eff})^3$. For u' values between 0.034 and 0.103, the Nusselt numbers obtained by our tests are practically merged with Eq. (1). Hahne's correlation (2) is checked only for $5 \times 10^4 < Gr_{gd_{eff}} Pr\, u' < 5 \times 10^5$, corresponding in our test conditions to $u' < 0.207$. It therefore cannot be used as a comparison with our tests at $u' = 0.69$. In its validity range correlation (2) gives Nusselt number values generally higher than ours, except for $u' = 0.24$, for which our experimental Nusselt number is very close to that one calculated by correlation (2). The fact that our test results are close to either correlation (1) or (2) validates our tests and proves that the slits in the fins a_1 and a_2 do not affect the convective heat transfer.

A last comparison can be obtained between our results and a correlation given by Elenbaas (1948), that allows to evaluate the heat transmission by natural convection between two vertical parallel disks of radius R_e at temperature T_s and spaced with a distance u:

$$Nu_u = \frac{h_m u}{\lambda_a} = \frac{Ra_u^+}{24}\left[1 - \exp\left(-\frac{35}{Ra_u^+}\right)\right]^{3/4},$$

where

$$Ra_u = Pr\ Gr_{gu} \quad \text{and} \quad Ra_u^+ = Ra_u \frac{u}{l_{eq}} \quad \text{with } l_{eq} = R_e \pi/2. \quad (3)$$

All the physical properties in this correlation, with the exception of β, are evaluated at the surface temperature T_s. The thermal expansion coefficient β is evaluated at T_∞. Eq. (3) is plotted in Fig. 6 under the form $Nu = f(u')$, by using $Gr_g = 1.35 \times 10^6$. Nusselt number Nu calculated by (3) increases as a function of u' more abruptly than on the fin. For $u' > 0.155$, it then becomes equal to the asymptotic value $Nu = 18$. This value corresponds to the Nusselt number obtained for a laminar flow on a single vertical disk cooled by natural convection. It is very close to the asymptotic value of the Nusselt number $Nu = 18.5$ obtained with our tests for $u' > 0.26$. Indeed, the same flow characteristics by natural convection are obtained on the single fin and the disk. The air flows upwards on the vertical surface, a laminar boundary layer developing from the surface bottom.

3.2. Analysis of the tests carried out with dominant rotational forced convection

In Fig. 5, the rotational forced convection has a great influence on the convective exchanges for every spacing above a rotational speed depending on the fin spacing, when compared with gravitational natural convection. The variation of the Nusselt number becomes a sharp function of the Reynolds number. For high speeds, the main part of the fluid is carried

along by the disk rotation. For a fixed value of the rotational speed, the heat transfer coefficient increases with fin spacing. The increase in Nu with u' is interpreted by the increase in the diameter of the solid-body rotation region (Fig. 2) with decreasing u'. Indeed, the base of the fin, largely insulated from the flow, does not contribute actively to the heat transfer. Moreover, for a given rotational speed, as the fin spacing decreases, the heat transfer coefficient decreases because of the interaction of the boundary layers developed on two adjacent fins. This interaction is at the origin of the decrease in the velocity gradients in the boundary layer, leading to a convective heat transfer drop on the fin. Furthermore, the central part becomes too small to maintain an efficient circulation when the boundary layers fill the largest part of the inter-fin space. For a given u' value, the heat transfer coefficient, with an increase in rotational speed, approaches the heat transfer coefficient for the single fin configuration. Indeed, the thickness of the boundary layer developed on the fins decreases with the increase in the rotational speed, thus favoring the fluid circulation and convective heat transfer from the fins. Moreover, with the increase in the Reynolds number, the flow becomes unsteady and 3D, which is favorable to the convective heat transfer.

3.3. Correlation of the tests

The Navier–Stokes, energy and continuity equations which are written under dimensionless form and applied to the air between two fins depend on the dimensionless numbers Re_ω and Gr_g. Moreover, geometrical parameters u', e' and H' are used to write the boundary conditions. The average Nusselt number on the fin is therefore expressed as a function of the dimensionless numbers Re_ω, Gr_g, u', e' and H'. In our tests, e' and H' values remain constant. Our tests which were carried out by natural, mixed or forced convection are accurately correlated with the following equation:

$$Nu = [A_2 Gr_g u'^{b_2} + 9.1 \times 10^{-3} X Re_\omega^2]^{0.275}$$

with

$$X = \left(\frac{e'}{u'} + 1\right)^2 \left(1 - \frac{K}{u'^b} Re_\omega^{-0.04}\right)^2. \quad (4)$$

The constant values K, b, A_2 and b_2 are given in Table 1 for $400 \leqslant Re_\omega \leqslant 30\,000$.

In Eq. (4), the numbers Gr_g and Re_ω^2 appear because the Navier–Stokes equations written under dimensionless form show that ratio Gr_g/Re_ω^2 gives a qualitative information on the influence of natural convection compared with rotational convection. By forced convection, the term X then expresses the ratio of the Nusselt number obtained for dimensionless fin spacing u' and the Nusselt number obtained on the single fin. This term increases with an increase in fin spacing or Reynolds number. Eq. (4) can also be used for lower Re_ω values by interpolation of the known values of the Nusselt number by natural convection and forced convection. This equation however can only be written for values of $Re_\omega > 150$, corresponding to $(K/u'^b)Re_\omega^{-0.04} < 1$.

Table 1
Constant values in Eq. (4)

	K	b
$0.034 \leqslant u' \leqslant 0.14$	0.844	0.11
$0.14 \leqslant u'$	0.394	0.5
	A_2	b_2
$0.034 \leqslant u' \leqslant 0.26$	0.39	1.92
$0.26 \leqslant u'$	0.03	0

The tests carried out with the rotating fins, correlated by Eq. (4) are plotted in Fig. 5, by using Grashof number $Gr_g = 1.35 \times 10^6$, for different u' values. Eq. (4) corresponds to our tests with a relative difference below 5%. The influence ranges of rotational forced convection and gravitational natural convection can be deduced from correlation (4). One obtains, for each spacing u, the value of ratio Re_ω^2/Gr_g, noted r_1, above which the influence of the natural convection is lower than 5% in the convective exchanges (Fig. 7(a)). r_1 increases as a function of u' until $u' \approx 0.24$ from $r_1 = 10.7$ to $r_1 = 64$ and r_1 decreases for $u' > 0.24$ approaching $r_1 = 17$, obtained for the single fin configuration. Similarly, the influence of the rotational forced convection is lower than 5% in the convective exchanges for ratio Re_ω^2/Gr_g lower than r_0 (Fig. 7(b)). r_0 increases as a function of u' until $u' \approx 0.24$ from $r_0 = 0.9$ to $r_0 = 2.85$. For $u' > 0.24$, r_0 decreases as a function of u' and approaches $r_0 = 0.63$, obtained for the single fin configuration. The Nusselt number values corresponding to the ratios Re_ω^2/Gr_g equal to r_1 and r_0, respectively, have been positioned in Fig. 5.

3.4. Comparison of total convective heat transfer from the finned tube and the smooth cylinder

The increase in the total convective heat transfer from the finned tube compared with that from the plain cylinder is evaluated in case the convective exchanges are controlled by rotational forced convection. The variation of the ratio of total convective heat flow ϕ_T dissipated by the finned tube surface and that dissipated by the smooth cylinder surface (outer diameter D) is studied as a function of the fin spacing and

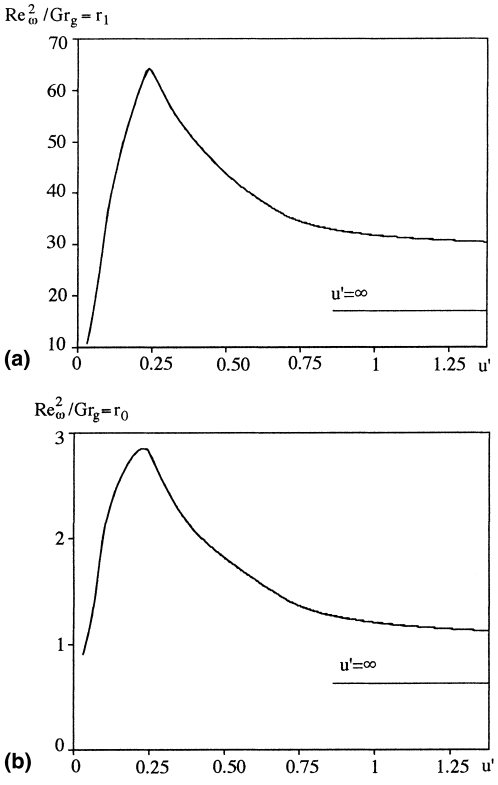

Fig. 7. (a) Variation of $Re_\omega^2/Gr_g = r_1$ as a function of u'. (b) Variation of $Re_\omega^2/Gr_g = r_0$ as a function of u'.

Reynolds number Re_ω. The total heat flow dissipated by the finned surface (Fig. 4) is

$$\phi_T = h_{red}(T_0 - T_\infty)S_1, \quad \text{where } h_{red} = h_m E\frac{S_a}{S_1} + h_0\frac{S_t}{S_1}. \tag{5}$$

S_1 represents the surface of the smooth cylinder; S_a and S_t represent the surface of fin in contact with the fluid and surface of the finned cylinder between the fins, respectively. Their expression as a function of the geometrical sizes of the finned tube is given in the nomenclature for circular fins of constant thickness. Thus, the reduced heat transfer coefficient h_{red} referred to S_1 is expressed as a function of the geometrical parameters of the finned tube by

$$h_{red} = h_m E\left(\frac{R_e^2 - R_i^2}{R_i s} + \frac{eR_e}{sR_i}\right) + h_0\frac{u}{s}. \tag{6}$$

The ratio of the convective heat flow ϕ_T dissipated by the finned tube surface and of that dissipated by the plain cylinder surface at temperature T_0 is equal to $h_{red}/h_1 = Nu_{red}/Nu_1$.

An estimate of the heat transfer coefficient, h_0, of the cylinder outer surface located between two fins is given by h_1 (heat transfer coefficient of the smooth cylinder). With the fin sizes used in our tests and the high thermal conductivity of the aluminum fins ($\lambda_{al} = 233$ W m^{-1} K^{-1}), the fin efficiency is estimated to be equal to $E = 0.93$. Eq. (6) is then written by replacing the constant geometrical sizes with their numerical values

$$h_{red} = 0.945\frac{h_m}{e' + u'} + \frac{u'}{e' + u'}h_1$$

or (7)

$$Nu_{red} = 0.945\frac{Nu}{e' + u'} + \frac{u'}{e' + u'}Nu_1.$$

To evaluate Nusselt number Nu at the fin surface, correlation (4) is used, with $Gr_g = 0$. To evaluate Nu_1, the correlation suggested by Kays and Bjorklund (1958) available within the range $600 < Re_\omega < 5 \times 10^4$, is used to calculate the convective heat transfer from a rotating heated cylinder to the air

$$Nu_1 = 0.18[(0.5Re_\omega^2)Pr]^{0.315}. \tag{8}$$

The evolution of ratio Nu_{red}/Nu_1 as a function of the fin spacing, for fixed Re values ($Re_\omega = 560$, 5.6×10^3 and 3.2×10^4) is shown in Fig. 8. For a given Reynolds number Re_ω, there is an optimal dimensionless fin spacing, u'_{pic}, corresponding to a maximal value of ratio Nu_{red}/Nu_1. As $u' < u'_{pic}$, Nu_{red}/Nu_1 decreases with the decrease in u', because the totality of the fluid kinetic energy is dissipated by friction on the fin surface and subsequently the flow velocity in the space between the fins, referred to a frame of reference rotating with angular speed ω, approaches 0. For $u' > u'_{pic}$, the decrease in Nu_{red}/Nu_1 observed as u' increases is due to the decrease in the convective exchange surface with the air, i.e. in the outer finned tube surface. For Reynolds number $Re_\omega = 5.6 \times 10^3$, ratio Nu_{red}/Nu_1 decreases from 8.7 to 2.1 as parameter u' varies from 0.034 to 0.69. For weak u' values ($u' = 0.034$ or 0.052), ratio Nu_{red}/Nu_1 is an increasing function of Re_ω. For ratio $u' = 0.034$, ratio Nu_{red}/Nu_1 varies from 6 to 9 with the increase of Re_ω from 560 to 3.2×10^4. For $u' > 0.1$, ratio Nu_{red}/Nu_1 is almost independent of Reynolds number Re_ω. The value of the optimal dimensionless fin spacing decreases from 0.04 to 0.01 with the increase of Re_ω from 560 to 32 000. This is because the interaction of the boundary layers decreases with the increase in Re_ω.

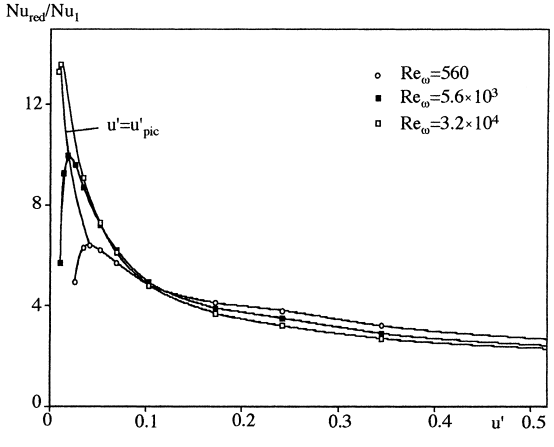

Fig. 8. Variation of Nu_{red}/Nu_1 as a function of u', for fixed Re_ω values.

4. Conclusion

The mean convective heat transfer from the central fin of a rotating finned tube has been obtained experimentally. The test results were plotted under the form of the average Nusselt number on the fin, as a function of the rotational Reynolds number (varying from 400 to 30 000), for different fin spacing values. For each spacing for the lowest rotational speeds, the heat transfer coefficient is independent of the rotational speed. In this case, the flow structure close to the fins is similar to that observed on fixed fins by natural convection and the influence of rotational convection is negligible on the convective heat transfer when compared with the gravitational natural convection. Our test results by natural convection are validated by comparing them with correlations found in the literature.

The rotational forced convection has a great influence on the convective exchanges for each spacing above a rotational speed, depending on the fin spacing, when compared with gravitational natural convection. By forced convection, the increase in Nu with u' is interpreted by the increase in the diameter of the solid-body rotation region with decreasing u'. Moreover, for a given rotational speed, as the fin spacing decreases the heat transfer coefficient decreases because of the interaction of the boundary layers developed on two adjacent fins and the central part becoming too small to maintain an efficient circulation. The heat transfer coefficient for a given u' value with an increase in rotational speed is close to the heat transfer coefficient for the single fin configuration. Indeed, the thickness of the boundary layer developed on the fins decreases with the increase in rotational speed, thus favoring fluid circulation. Moreover, with the increase in the Reynolds number, the flow becomes unsteady and 3D, which is favorable to the convective heat transfer.

All the tests carried out with rotating fins, a dimensionless fin spacing between 0.034 and 0.69 and a tube with a single fin are correlated with a general equation with a relative difference below 5%. This equation expresses the average Nusselt number on the fin as a function of the Reynolds number Re_ω, Grashof number Gr_g and dimensionless fin spacing u'. The influence ranges of rotational forced convection and gravitational natural convection on the convective exchanges are deduced from the correlation obtained. The convective exchanges are controlled by gravitational natural convection when $Re_\omega^2/Gr_g < r_0$ with r_0 between 0.6 and 2.85 and by rotational convection when $Re_\omega^2/Gr_g > r_1$ with r_1 between 11 and 64.

The study of the variation of the convective heat transfer's ratio from the surface of the finned tube and the isolated cylinder surface ($= Nu_{red}/Nu_1$) shows the increase of the convective exchanges from the finned surface. For ratio $u' = 0.034$,

when rotational Reynolds number Re_ω controls the heat transfer, ratio Nu_{red}/Nu_1 varies from 6 to 9 with the increase in Re_ω from 600 to 3.2×10^4.

References

Abrahamson, S., Eaton, J., Koga, D., 1989. The flow between shrouded corotating disks. Phys. Fluids A 1, 241–251.

Akhmetov, D.G., Tarasov, V.F., 1987. J. Appl. Mech. Tech. Phys. 27, 690.

Chang, C.J., Schuler, C.A., Humphrey, J.A.C., Greif, R., 1989. Flow and heat transfer in the space between two corotating disks in an axisymmetric enclosure. J. Heat Transfer, Trans. ASME 111, 625–632.

Elenbaas, W., 1948. Dissipation of heat by free convection. Parts I et II, Philips Research Report 3. N.V. Philips' Gloeilampenfabrieken, Eindhoben, Netherlands, pp. 338–60 et 450–465.

Hahne, E., Zhu, D., 1994. Natural convection heat transfer on finned tubes in air. Int. J. Heat Mass Transfer 37 (1), 59–63.

Herrero, J., Giralt, F., Humphrey, J.A.C., 1999. Influence of the geometry on the structure of the flow between a pair of corotating disks. Phys. Fluids 11 (1), 88–96.

Kays, W.M., Bjorklund, I.S., 1958. Heat transfer from a rotating cylinder with and without crossflow. Trans. Am. Soc. Mech. Eng. 170, 70–78.

Lennemann, E., 1974. Aerodynamic aspects of disk files. IBM J. Res. Develop. 18 (6), 480–488.

Murthy, J.Y., 1988. Study of heat transfer from a finned rotating cylinder. J. Thermophys. 2 (3), 250–256.

Schuler, C.A., Usry, W., Weber, B., Humphrey, J.A.C., Greif, R., 1990. On the flow in the unobstructed space between shrouded corotating disks. Phys. Fluids A 2, 1760.

Stewartson, K., 1957. On almost rigid rotations. J. Fluid Mech. 3, 17.

VDI-Wärmeatlas, 1991. Sechste erweiterte Auflage, Fa5, Fa6.

Watel, B., Harmand, S., Desmet, B., 1994. Etude de faisabilité du refroidissement d'un disque de frein équipé d'un caloduc. Entropie 187, 25–37.

Watel, B., Harmand, S., Desmet, B., 1995. Etude expérimentale de faisabilité du refroidissement d'un disque de frein équipé d'un caloduc. Entropie 191, 25–33.

Watel, B., Harmand, S., Desmet, B., 1998. Etude des échanges convectifs sur un arbre aileté tournant, soumis à un courant d'air parallèle aux ailettes. Int. J. Heat Mass Transfer 41, 3741–3757.